Supplementary Materials for

Glutamate-Dependent Neuroglial Calcium Signaling Differs Between Young and Adult Brain

Wei Sun, Evan McConnell, Jean-Francois Pare, Qiwu Xu, Michael Chen, Weiguo Peng, Ditte Lovatt, Xiaoning Han, Yoland Smith, Maiken Nedergaard*

*To whom correspondence should be addressed. E-mail: nedergaard@URMC.Rochester.edu

Published 11 January 2013, *Science* **339**, 197 (2013)
DOI: 10.1126/science.1226740

This PDF file includes:

Supplementary Material 1226740 by Sun et al.

1. Materials and Methods

Human and mouse tissue samples

Human cortical tissue was obtained from surgical specimens from one female and two male adolescence patients all having hippocampal malformations and absence of gliosis in the surgically removed cortical tissue. Tissue samples were collected with informed consent and tissue donation approval under protocols approved by the Research Subjects Review Board of the University of Rochester Medical Center. Mouse parietal cortex or hippocampus samples were harvested from 1, 2, 3, or 12 weeks old male C57BL/6 mice. A subset of experiments used *Aldh1l1-EGFP reporter* mice on C57BL/6 background (*1, 2*).

Dissociation of human and mouse brain tissue followed by FACS

Dissociation of the human and mouse cortical tissue was performed as described previously (*3, 4*) with minor modifications. Mice were anesthetized with pentobarbital (50 mg kg^{-1}, i.p.), perfused with cold Hanks buffer and decapitated. The brain was immediately removed and parietal cortex or hippocampus was dissected and cut into small pieces, which were digested with 5 U/ml papain in Ca^{2+}/Mg^{2+}-free PIPES/cysteine buffer, pH 7.4, for 1 h at 37°C/5% CO_2. After one wash, the tissue was then further digested with 40 U/ml DNase I in Mg^{2+}-containing MEM with 1% bovine serum albumin (BSA) for 15 min at 37°C/5% CO_2. The tissue was then carefully triturated in cold MEM with 1% BSA, centrifuged over a 90% Percoll gradient. Cells below and included in the lipid layer were collected followed by centrifuged to collect the pellet. The cells were labeled with rabbit anti-GLT1 antibody (1:150, custom made) or rabbit IgG control followed by labeling with secondary donkey anti-rabbit Allophycocyanin (APC) (1:200). Cells were resuspended in cold MEM with 1% BSA containing 5ug/ml 4',6-diamidino-2-phenylindole DAPI to discriminate dead cells.

Cells were sorted using Fluorescent Activated Cell Sorting (FACS). Single cells were discriminated using pulse width and height measurements. APC was excited by a 633 nm laser, and emissions were collected by a 660/20nm band-pass filter. DAPI was excited by a 407 nm laser and emissions were collected by a 450/40 band-pass filter. Dead cells were excluded according to positive DAPI signal. GLT1+ and GLT1- populations were gated according to isotype control. Cells were sorted into cold MEM containing 1% BSA. To isolate ALDH1L1+ cells, cortices and hippocampus from Aldhl1l-EGFP mice were dissociated and purified into ALDH1L1+ and ALDH1L1- pools using FACS.

RNA processing, microarray, and quantitative PCR

After FACS, cells were immediately extracted for total RNA using either the RNAqueous Micro kit or RNeasy Micro Kit. RNA quantity was assessed using the NanoDrop-1000, and RNA integrity was assessed using the 2100-Bioanalyzer. For microarray, 20 ng of total RNA was amplified and labeled with biotin using the Ovation kit according to the manufacturer's instruction and hybridized to Human U133+ 2.0 or Mouse Genome 430 2.0 Array. For quantitative PCR (qPCR), total RNA was reverse transcribed and amplified. Relative quantity of transcripts was assessed using Taqman Assays on Demand and the 7000 Sequence Detection System. 18S RNA served as an internal control that all samples were normalized to before calculating relative expression to mGluR1.

Microarray data analysis

Microarray data were analyzed using the GeneSpring GX Software. We normalized the data using the MAS5 algorithm. To assure reproducibility among independent biological replicates in the genomic data set, we compared the correlation coefficient within groups of sorted cells. The degree of similarity across all samples was assessed by hierarchical clustering using Euclidean average distances. Arbitrary units of signal intensities were used to screen the mGluRs expression by astrocytes.

Immunocytochemistry

FACS isolated cells were plated in poly-D-lysine coated 24-well plate, fixed with 4% paraformaldehyde as soon as adherent (~10-20 min), and labeled with mouse anti-AQP4 or mouse anti-ALDH1L1, followed by labeling with Alexa 555-conjugated donkey anti-mouse IgG and DAPI. The cells were then visualized and quantified under an inverted fluorescent microscope.

Preparation of acute cortical and hippocampal slices

Unless otherwise noted, 12-15 day old C57BL/6 or GLT1-EGFP reporter mice (on C57BL/6 background, (*5*) were used for preparation of cortical or hippocampal slices as previously described (*6*). The pups were anesthetized in a closed chamber with isofluorane (1.5%), and decapitated. The brains were rapidly removed and immersed in ice-cold cutting solution that contained (in mM): 230 sucrose, 2.5 KCl, 0.5 $CaCl_2$, 10 $MgCl_2$, 26 $NaHCO_3$, 1.25

NaH_2PO_4, and 10 glucose, pH=7.2-7.4. Coronal slices (400 µm) were cut using a vibratome and transferred to oxygenated aCSF that contained (in mM): 126 NaCl, 4 KCl, 2 $CaCl_2$, 1 $MgCl_2$, 26 $NaHCO_3$, 1.25 NaH_2PO_4, and 10 glucose, pH = 7.2-7.4, osmolarity 310 mOsm. Slices were incubated in aCSF for 1 hour at room temperature before 15-25 min loading with rhod-2 AM (5 µM). Experiments were performed at room temperature (21-23 ºC). The slices were placed in a chamber at the microscope stage and superfused with aCSF gassed with 5% CO_2 and 95% O_2 at room temperature. Cells were visualized with a 40X water-immersion objective and differential inference contrast (DIC) optics.

Animal preparation for in vivo 2-photon imaging

C57BL/6, GLT1-EGFP reporter mice (on C57BL/6 background (*5*)); either 12-15 days old or adult (10-12 weeks), were anesthetized with an intraperitoneal injection of ketamine (0.12 mg g^{-1}) and xylazine (0.01 mg g^{-1}). Depth of anesthesia was monitored by pinch withdrawal and anesthesia was supplemented with half the initial dose of ketamine and xylazine every hour or sooner if the mice responded to pinch stimulation. Body temperature was maintained at 37°C by a heating blanket. The mice were intubated and artificially ventilated with a small animal ventilator. Blood was taken through a femoral artery catheter and pCO_2, pO_2 and pH were analyzed in microsamples. Experiments were completed only if physiological variables remained within normal limits. The normal limits for pCO_2 were set at 35–45 mm Hg; pO_2, 80–115 mm Hg; and arterial blood pH, 7.35–7.45. A craniotomy (2–3 mm in diameter), centered 0.5 mm posterior to the bregma and 3.5 mm lateral from midline, was made over the right primary somatosensory cortex, and the dura removed. A custom-made metal plate was glued to the skull with dental acrylic cement. Rhod-2/am (10 µM) was dissolved in dimethylsulfoxide (DMSO) with 20% pluronic acid and mixed in artificial cerebrospinal fluid (aCSF) containing 126 mM NaCl, 2.5 mM KCl, 1.25 mM NaH_2PO_4, 2 mM $MgCl_2$, 2 mM $CaCl_2$, 10 mM glucose and 26 mM $NaHCO_3$ (pH 7.4), gassed with 95% O_2 and 5% CO_2 at 37 °C (*7*). After 15-25-min loading, the exposed brain was washed for 15 min with aCSF without dye. Agarose (1%, 37 °C) was poured on the cranial window and the glass coverslip was glued to the metal plate with dental acrylic cement. In a subset of animals, t-ACPD (500 µM) induced Ca^{2+} responses were analyzed in awake mice. In these experiments, the mice were trained in multiple ~30 min lasting sessions to head restraining at the microscope stage. At the day of the experiment, the cranial window was prepared in isoflurane anesthetized mice. The animals were after rhod2 AM loading allowed to wake up for 1 hr prior to imaging, as previously described (*8*).

In vivo two-photon imaging

A custom-built microscope attached to Tsunami/Millinium laser (10 W) and a scanning box using Fluoview software and a 20 × objective (0.9 NA) was used for two-photon imaging. Excitation wavelength was in the range of 820–840 nm. Two-channel detection of emission wavelength was achieved by using a 565-nm dichroic mirror and two external photomultiplier tubes. A 620/60 filter was used to detect rhod-2 AM emission wavelength. Time-lapse images of astrocytic Ca^{2+} signaling were recorded every 1 s. The two-photon laser power was adjusted daily to an average power that was less than 30 mW at the cortical surface to avoid photo damage.

Agonist microinjections and quantification of agonist-induced Ca^{2+} signaling and EEG

Astrocytic Ca^{2+} signaling was induced by puffing of aCSF containing the agonists at a depth of ~100 μm below the surface in cortical and hippocampal slices or ~100 below the pia surface (cortical layer II) in live imaging experiments. The micropipettes where filed with aCSF containing Alexa 488 (100μM) to visualize agonist delivery using picospritzer III (50 msec duration, 10 psi). Agonists including dihydroxyphehylgycine (DHPG, 200μM), (±)-1-Aminocyclopentane-*trans*-1,3-dicarboxylic acid (tACPD, 500μM), (RS)-2-chloro-5-hydroxyphenylglycine (CHPG, 500 μM), adenosine triphosphate (ATP, 500μM), N-acetylaspartylglutamate (NAAG, 1mM), and LY379268 (100 μM). Number of responding cells was quantified by counting the number of cells that displayed increases intracellular Ca^{2+} (rhod-2 emission signal) higher than two standard deviations above baseline in response to agonist application (*8*). The baseline was measured as the mean intensity of frames preceding the application of agonist. Standard deviation was calculated in individual by measured rhod-2 signal using a circular region of interest in Imagej64. On average 25-50 cells per mouse were assessed. The velocities of Ca^{2+} waves and Alexa 488 diffusion were measured as the distance traveled by the front of the wave divided by time elapsed. Ca^{2+} wave amplitudes were measured by calculating the difference between pre- and post-agonist stimulation followed by normalizing to the pre-agonist intensity levels (ΔF/F). Duration of agonist-induced Ca^{2+} transients was measured as the time spent above two standard deviations of the mean of the baseline. The diffusion velocity of Alexa 488 was used an internal control for the consistency of agonist application. Cortical EEG was recorded using injection electrode filled with aCSF or agonists. The electrode was inserted into cortical layer 2 and P-clamp used for the recordings. Power spectrum

analysis of EEG traces was done using Clampfit software. The first five seconds before and after agonist injection was used for the analysis. Power spectrum was displayed as % power calculated by the formula: power of spectral band / total power.

Animal preparation for immuno EM studies

A total of 6 adult mice were used in the electron microscopic studies. These animals were perfusion-fixed with a mixture of 4% paraformaldehyde and 0.1% glutaraldehyde fixative. Their brains were removed from the skull, postfixed in 4% paraformaldehyde for 24 hours, sectioned in 60 um-thick sections with a vibrating microtome, serially collected in PBS, and processed for the immunoperoxidase localization of mGluR5 and mGluR2/3 using the avidin biotin-peroxidase method and highly specific antibodies that have been thoroughly characterized in our laboratory and others (*9, 10*). After having been processed for EM according to procedures described in many of our previous studies (*9, 11*), 3 blocks of tissue from the cerebral cortex or hippocampus from each animal were taken out from the slides, cut in ultrathin sections with an ultramicrotome, mounted on single slots cupper grids, and analyzed with an electron microscope. From each of these blocks, 50 micrographs of randomly selected immunoreactive elements were taken at 16 000X so that a total of 2215 μm^2 of tissue area was analyzed from each region. In each micrograph, labeled elements were categorized as post-synaptic (neuronal cell bodies, dendrites, spines) or pre-synaptic (axons, terminals) neuronal elements or astrocytic processes based on specific ultrastructural features (*12*). The relative percentages of each of the three groups of labeled structures were then calculated and presented (Fig 3).

All experiments were approved by the Institution Animal Care and Use Committee of the Universities of Rochester and Emory.

2. Supplementary Figures

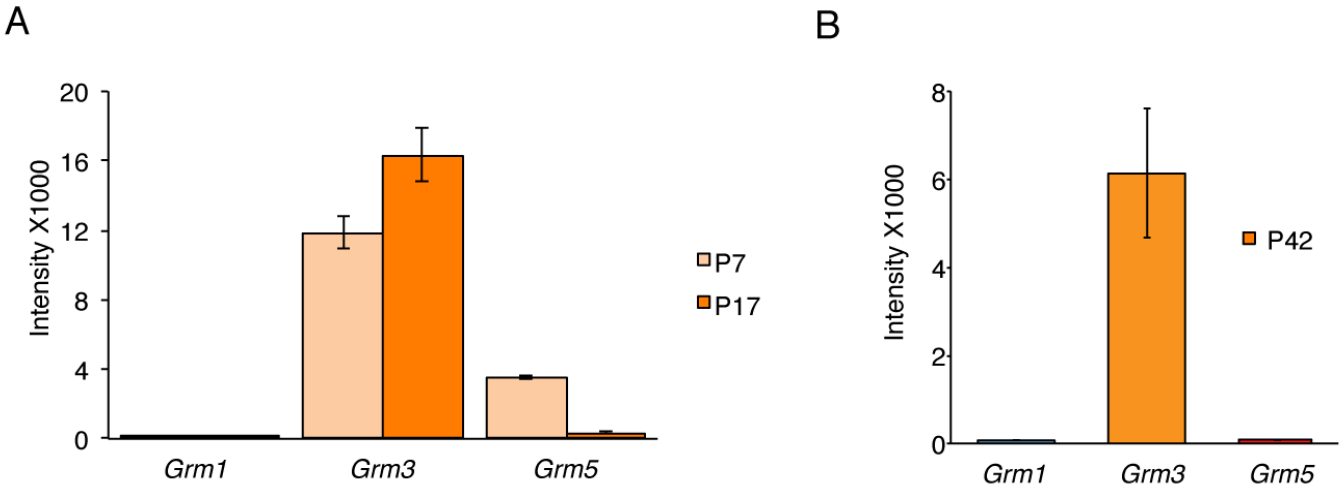

Fig. S1. Astrocytic expression of Group I and II mGluR based on analysis of published transcriptome data. (A) Forebrain astrocytes acutely isolated by FACS isolation in S100-EGFP mice followed by RNA extraction and microarray analysis shows that mGluR5 is down-regulated at postnatal day 17 (P17) compared to postnatal day 7 (P7). In comparison, mGluR3 is relatively stable expressed (n = 3, Mean ± SEM) (*2*). (**B**) mGluR3 is the major mGluR expressed by 6 weeks old cortical astrocytes based on the BAC-TRAP technique in which RNA was isolated from transgenic mice expressing EGFP-tagged ribosomal protein L10 driven by the astrocyte specific promoter Aldh1L1 (n = 3, Mean ± SEM) (*13*) (*2*).

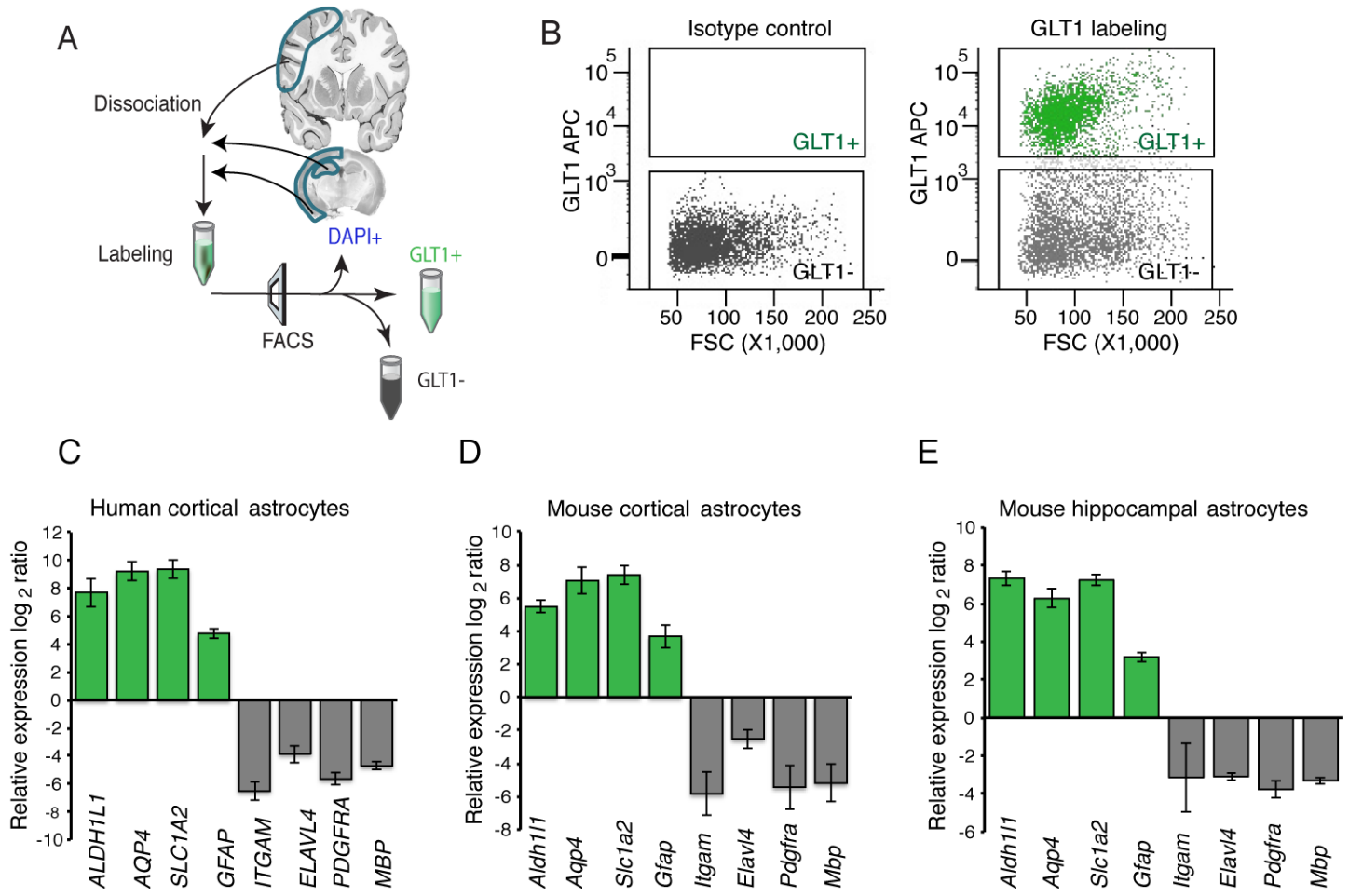

Fig. S2. Isolation and extraction of RNA from adult human and mouse astrocytes

(**A**) Schematic outline of astrocytes isolation. Brain tissue was dissociated, immunolabeled against RbGLT1-Allophycocyanin (APC), and sorted into GLT1+ and GLT1- cell populations by fluorescence activated cell sorting (FACS). (**B**) Plots of FACS purification of astrocytes. X-axis represents forward scatter; Y-axis represents APC fluorescent intensity. (***left panel***) Gating of GLT1- population was based on cells immunolabeled with an isotype control antibody**,** in which over 99% of cells fall into the GLT- gate. (***right panel***) Cells fall into the GLT1+ gate and GLT1- gate after GLT1 labeling were purified. (**C, D, E**) QPCR analysis of markers expression in purified human and mouse GLT1+ population: Compared to the median of both GLT1+ and GLT1- population, astrocytic specific markers, including aldehyde dehydrogenase 1 family, member L1 (*Aldh1l1*), aquaporin 4 (*Aqp4*), excitatory amino acid transporter 2 (*Slc1a2*) and glial fibrillary acidic protein (*Gfap*), are enriched in the GLT1+ population. Conversely, the GLT1+ population is depleted of the microglial marker, integrin alpha M (*Itgam*), the neuronal marker, HU-antigen D (*Elavl4*), the oligodendrocyte precursor marker, platelet derived growth factor receptor, alpha polypeptide (*Pdgfra*), and *the* oligodendrocyte marker, myelin basic protein *Mbp*). Error bar, standard deviation of the mean, n=3 biological replicates.

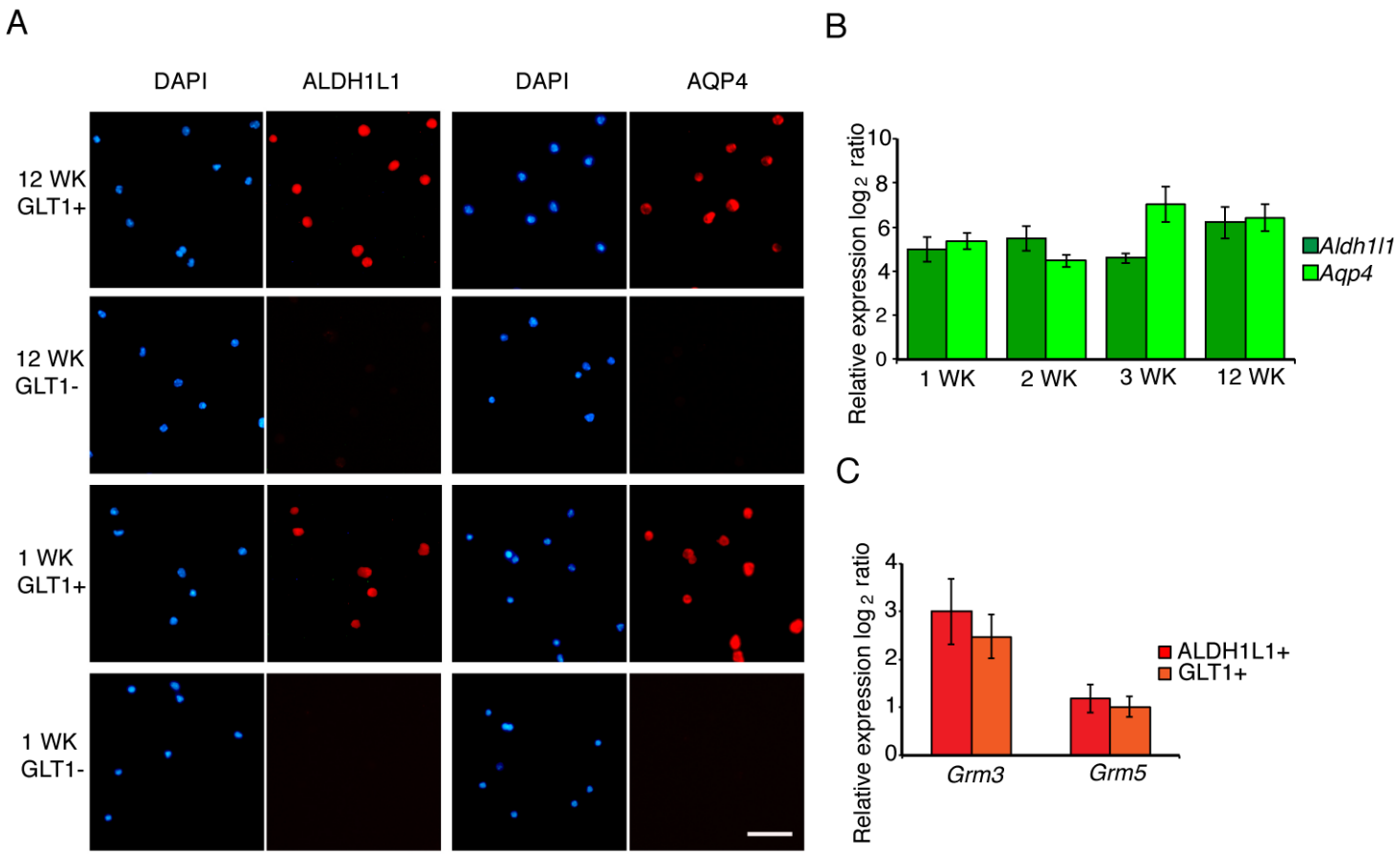

Fig. S3. Characterization of the GLT1+ population isolated by FACS.

(A) Sorted cells were examined by immunocytochemistry for astrocyte specific markers ALDH1L1 and AQP4 (red). DAPI (blue) was used to label all cells. At both 1 week and 12 week, GLT1+ cells are positive for ALDH1L1 (93.8% ± 2.5% at 1 WK and 96.7% ± 2.1% at 12 WK) and AQP4 (98%% ± 1.9% at 1 WK and 98.7% ± 1.1% at 12 WK), while GLT1- cells are depleted of ALDH1L1 (5.8%±2.5% at 1 WK and 1.4% ± 1.6% at 12 WK) and AQP4 (2.5% ± 0.5% at 1 WK and 0.6% ± 1% at 3 WK). (B) QPCR analysis of *Aldh1l1* and *Aqp4* mRNA expression in GLT1+ cells compared to GLT1- cells isolated at 1 week, 2 week, 3 week and 12 week. The enrichment of *Aldh1l1* and *Aqp4* transcripts are consistent from 1 week to 12 week. Error bar, standard deviation of the mean, n=3 biological replicates. (C) QPCR analysis of *Grm3* and *Grm5* expression in ALDH1L1-EGFP+ astrocytes and GLT1+ astrocytes isolated from 1 week old mice. No difference in either *Grm3* or *Grm5* expression between astrocytes isolated according to ALDH1L1 expression and GLT1 expression was identified. Error bar, standard deviation of the mean, n=3 biological replicates.

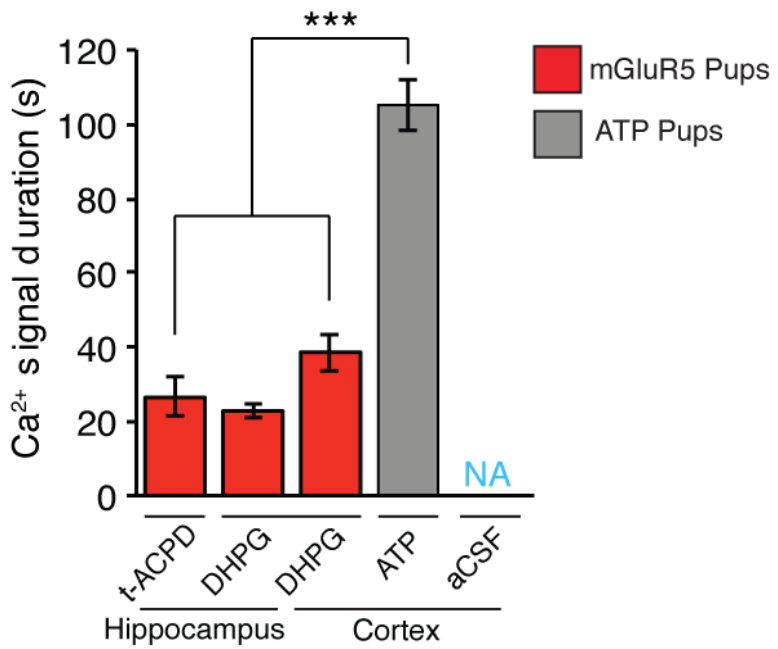

Fig. S4. Duration of agonist-induced astrocytic Ca^{2+} increases in hippocampal and cortical slices. The duration of Ca^{2+} increases induced by DHPG (200 µM), t-ACPD (500 µM), ATP (500 µM) was measured as the time in which the Ca^{2+} remains above 2 standard deviations above baseline. The duration of t-ACPD and DHPG induced Ca^{2+} increases did not differ ($p > 0.05$). The duration of ATP-induced Ca^{2+} increases were significantly longer that those induced by t-ACPD and DHPG (***, $p < 0.001$), ANOVA $p < 0.001$, $F = 18.3$.

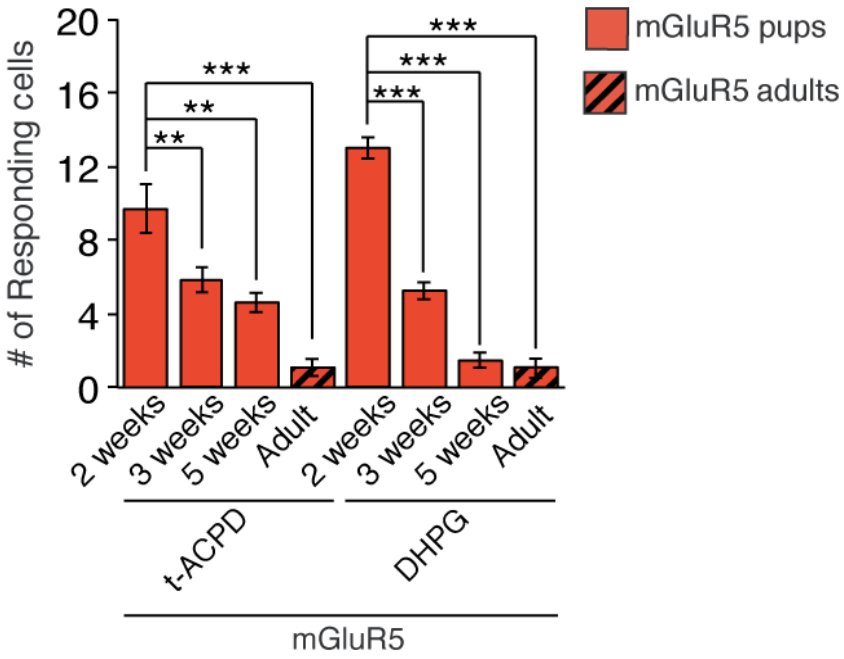

Fig. S5.Developmental down-regulation of mGluR5-induced Ca^{2+} signaling in cortical astrocytes in vivo
Number of astrocytes activated by micro-injection of t-ACPD (500 µM) and DHPG (200 µM) plotted as a function of the age of the animals. *p < 0.05, 5 weeks vs. 2 weeks, *p <0.05, and 8 weeks vs 2 weeks, ***p < 0.001 . ANOVA p < 0.001, F = 20.62. For DHPG all subsequent aged animals were significantly different from 2 weeks, ***p < 0.001, ANOVA p < 0.001, F = 103.

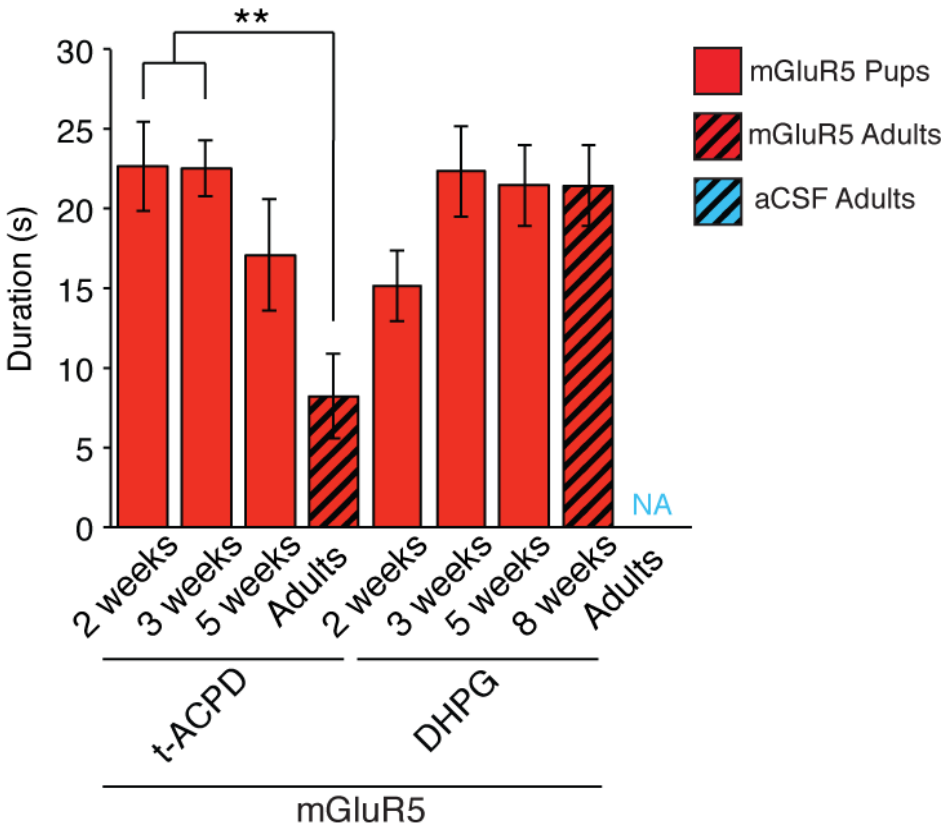

Fig. S6. Duration of agonist-induced astrocytic Ca^{2+} increases in vivo.

Duration of t-ACPD (500 µM), DHPG (200 µM), CHPG (500 µM), and ATP (500 µM) induced Ca^{2+} signals in pups and adult mice vivo. The duration of Ca^{2+} increases was measured as the time in which the Ca^{2+} remains above 2 standard deviations above baseline. **$p < 0.01$. ANOVA $p < 0.01$, $F = 7.1$

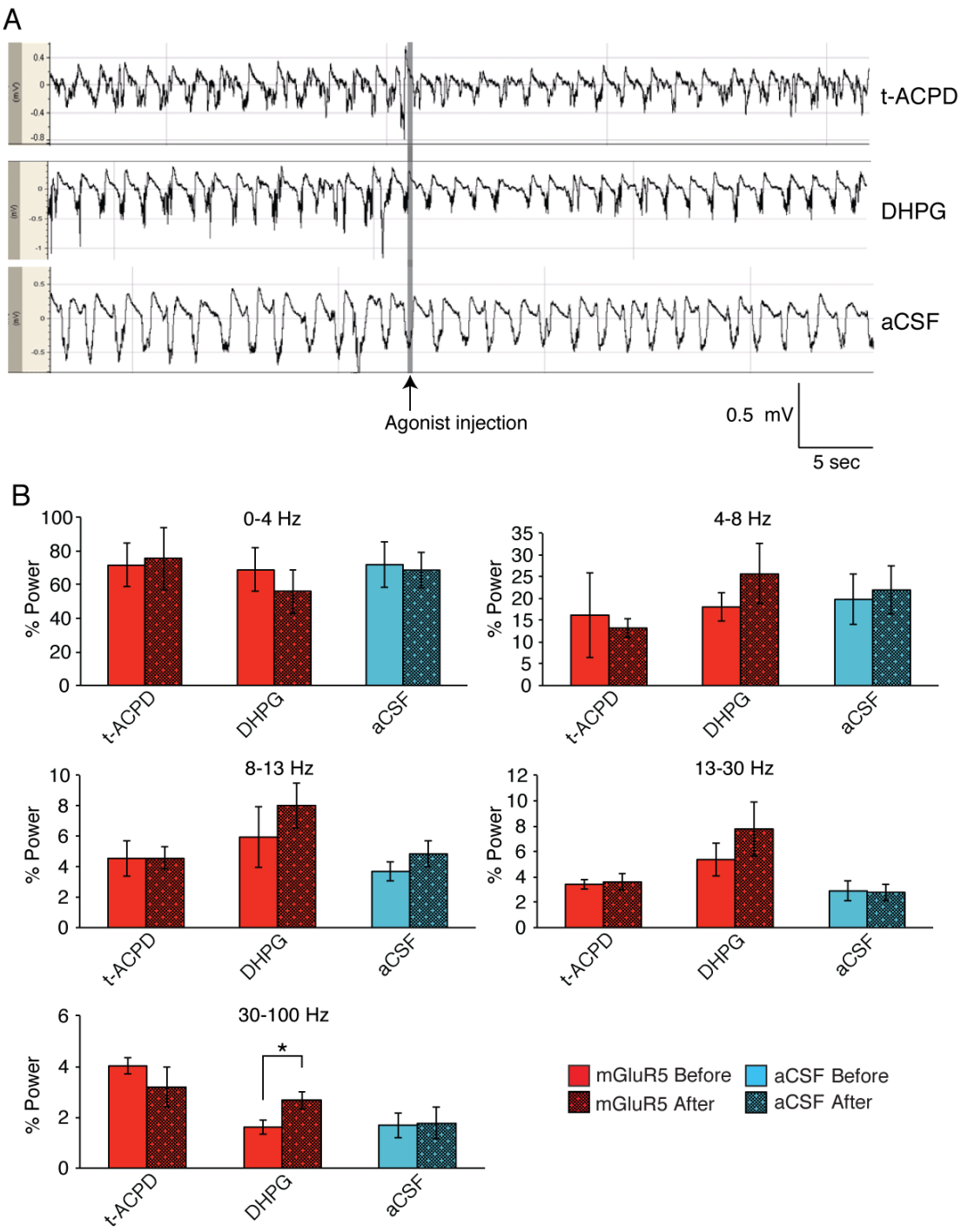

Fig S7. Effect of local injection of mGluR5 agonist, t-ACPD (500 µM), DHPG (200 µM) or vehicle (aCSF) on EEG in adult anesthetized mice. (**A**) Raw traces of EEG recordings before and during local administration of either t-ACPD, DHPG, or vehicle. (**B**) Power spectrum analysis of the EEG recordings showed no significant change before or during agonists or aCSF injections in delta (0-4Hz), theta (4 – 8 Hz), alpha (8 – 13 Hz), or beta bands (13 – 30 Hz) ($p > 0.05$, two tailed student t-test). However, DHPG significantly increased high frequency gamma signals ($p < 0.05$, two tailed student t-test, mean ±SEM, n = 10).

References and Notes

1. Y. Zhang, B. A. Barres, Astrocyte heterogeneity: an underappreciated topic in neurobiology. *Curr Opin Neurobiol* **20**, 588 (Oct, 2010).
2. J. D. Cahoy *et al.*, A transcriptome database for astrocytes, neurons, and oligodendrocytes: a new resource for understanding brain development and function. *J Neurosci* **28**, 264 (Jan 2, 2008).
3. D. Lovatt *et al.*, The transcriptome and metabolic gene signature of protoplasmic astrocytes in the adult murine cortex. *J Neurosci* **27**, 12255 (Nov 7, 2007).
4. F. J. Sim *et al.*, CD140a identifies a population of highly myelinogenic, migration-competent and efficiently engrafting human oligodendrocyte progenitor cells. *Nature biotechnology* **29**, 934 (Oct, 2011).
5. M. R. Regan *et al.*, Variations in promoter activity reveal a differential expression and physiology of glutamate transporters by glia in the developing and mature CNS. *J Neurosci* **27**, 6607 (Jun 20, 2007).
6. A. Torres *et al.*, Extracellular Ca2+ acts as a mediator of communication from neurons to glia. *Science signaling* **5**, ra8 (2012).
7. F. Wang *et al.*, Astrocytes modulate neural network activity by Ca(2)(+)-dependent uptake of extracellular K(+). *Science signaling* **5**, ra26 (Apr 3, 2012).
8. A. S. Thrane *et al.*, General anesthesia selectively disrupts astrocyte calcium signaling in the awake mouse cortex. *PNAS*, (in press) (2012).
9. M. Kuwajima, R. A. Hall, A. Aiba, Y. Smith, Subcellular and subsynaptic localization of group I metabotropic glutamate receptors in the monkey subthalamic nucleus. *The Journal of comparative neurology* **474**, 589 (Jul 5, 2004).
10. R. S. Petralia, Y. X. Wang, A. S. Niedzielski, R. J. Wenthold, The metabotropic glutamate receptors, mGluR2 and mGluR3, show unique postsynaptic, presynaptic and glial localizations. *Neuroscience* **71**, 949 (Apr, 1996).
11. Y. Smith, J. Bolam, in *Experimental Neuroanatomy: A practical approach,* J. P. Bolam, Ed. (Oxford University Press, Oxford, UK, 1992), pp. 239-266.
12. Peters A, Palay SL, Webster HD, *The fine structure of the nervous system : neurons and their supporting cells*. (Oxford University Press, New York, 1991), vol. xviii.
13. J. P. Doyle *et al.*, Application of a translational profiling approach for the comparative analysis of CNS cell types. *Cell* **135**, 749 (Nov 14, 2008).